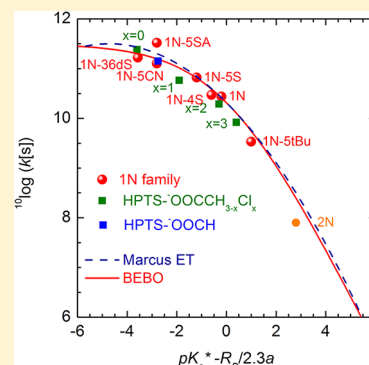


## Ultrafast Excited-State Proton-Transfer Reaction of 1-Naphthol-3,6-Disulfonate and Several 5-Substituted 1-Naphthol Derivatives

Mirabelle Prémont-Schwarz,<sup>†</sup> Tamar Barak,<sup>‡</sup> Dina Pines,<sup>‡</sup> Erik T. J. Nibbering,<sup>\*,†</sup> and Ehud Pines<sup>\*,‡</sup><sup>†</sup>Max-Born-Institut für Nichtlineare Optik und Kurzzeitspektroskopie, Max-Born-Str. 2 A, D-12489 Berlin, Germany<sup>‡</sup>Department of Chemistry, Ben-Gurion University of the Negev, P.O.B. 653, Beer-Sheva 84105, Israel

**ABSTRACT:** The 1-naphthol molecule has been the subject of intense research activity for the past 60 years due to its complex behavior as a photoacid upon optical excitation. We have utilized femtosecond mid-infrared spectroscopy and time-resolved fluorescence spectroscopy to investigate the excited-state proton-transfer reaction of 1-naphthol-3,6-disulfonate (1N-3,6diS) and several 5-substituted 1-naphthol derivatives. The proton dissociation rate constant of 1N-3,6-diS was found to be about 3 times faster and the  $pK_a^*$  about 2  $pK_a$  units more acidic than the values previously reported in the literature. A Marcus (free-energy) plot of excited-state proton dissociation rate constants vs the excited-state equilibrium constant of the photoacids,  $K_a^*$ , was constructed using the C-5 series of 1-naphthol derivatives. The newly measured values for the ESPT rate constant and  $pK_a^*$  of 1N-3,6diS was found to fit well with the Marcus correlation. We discuss our findings in the context of the photoacidity phenomenon in general, and the photoacidity of 1-naphthol and its derivatives in particular.



## 1. INTRODUCTION

Aromatic molecules containing acidic or basic functional groups, such as alcohols or amines, are found to show remarkable changes in acidity upon excitation to their first electronic excited singlet state ( $S_1$ ). In particular, weak ground-state Brønsted acids<sup>1,2</sup> such as hydroxyaromatics become much stronger acids, often capable of undergoing excited-state proton-transfer reactions to water or to an accepting base. This phenomenon is usually referred to as photoacidity, and the molecules named photoacids.<sup>3–5</sup> Arguably, the first report on a proton-transfer reaction initiated by absorption of light was made by Weber<sup>6</sup> and later by Terenin.<sup>7</sup> The photoacidity phenomenon of organic dyes was first described by Förster<sup>8,9</sup> who correctly interpreted the large Stokes shift observed in the fluorescence spectra of photoacids as emerging not from the acid, but instead from its conjugate that is generated following rapid (picosecond to nanosecond) proton dissociation from the acid. This proton-transfer reaction from photoacids in aqueous solution occurring within the short span of their excited-state lifetime has become the most researched aspect of photoacidity.<sup>8–16</sup> Ultrafast electronic spectroscopy using UV/vis pump–probe, fluorescence up-conversion and time-correlated single photon counting techniques have been utilized to monitor excited-state proton-transfer dynamics in real-time.<sup>17–28</sup> Rates of the excited-state proton-transfer (ESPT) reaction to the solvent have been derived using kinetic modeling of the observed transient signals. Free-energy reactivity correlation plots have been reported which connect proton-transfer reaction rates with  $pK_a^*$  values.<sup>15,29–33</sup> More recently, femtosecond mid-infrared (mid-IR) absorption spectroscopy has been utilized to follow the pathway of the proton

in real time from photoacids to water or to proton acceptors such as carboxylate bases.<sup>33–49</sup>

Photoacidity has been shown to depend both on the electronic structure of the chromophore and on the solvent. The first clear demonstration of the interplay between the solvent and excited-state proton transfer was reported by Paul F. Barbara's group who investigated the dynamics of the intramolecular proton-transfer reaction of photoexcited hydroxyflavones.<sup>50–53</sup> It was found that the intramolecular excited-state proton-transfer reaction was noticeably slower, or even entirely blocked, in solvents that formed competing (intermolecular) hydrogen bonds with the photoacid. Indeed, in a similar manner as that found in ground-state (Brønsted) acids,<sup>1,2</sup> the acid–base equilibria of photoacids and the proton dissociation (and recombination) rates are controlled by the solvent.<sup>16</sup> The generalized kinetic model for acid–base reactions in solution with the solvent interacting dynamically with the acid, conjugated base, and proton was mainly developed by Eigen<sup>54,55</sup> and Weller.<sup>10,56,57</sup> In addition, solvent relaxation around the excited photoacid may affect and limit the rate of intramolecular charge redistribution processes within the excited photoacid system. This aspect of the solvent-photoacid interaction has been the subject of intense examination and debate and is considered an important factor in determining if the photoacid is able to dissociate within the short lifetime of the excited state.<sup>16,28,58</sup>

**Special Issue:** Paul F. Barbara Memorial Issue

**Received:** September 3, 2012

**Revised:** December 23, 2012

**Published:** January 10, 2013

Though much research has been devoted to clarifying and characterizing the role of the solvent in photoacidity, the effect of the electronic structure of the chromophore has received much less attention. One of the first photoacids to be investigated was 1-naphthol,<sup>3,4,8,11,57,59–62</sup> which has become a prototype photoacid as it demonstrates the full richness and complexity of the photoacidity phenomena. The complex photophysics of 1-naphthol was suggested to be associated with both intramolecular charge-transfer processes following photoexcitation, and dynamic solvent–solute interactions.<sup>3,4</sup> Additional aspects of the complex electronic structure of 1-naphthol has come to light when it was found that protons readily quench the excited electronic state of 1-naphthol and 1-naphtholate anion.<sup>63,64</sup>

In this contribution, the effect of substituents on the photoacidity of 1-naphthol was studied. In the ground state, the electron-donating or electron-withdrawing strength of groups on aromatic molecules has been traditionally quantified by the Hammett  $\sigma$  value of the substituent. We have analyzed the substituent effect of electron-withdrawing and -donating groups at the 5 position (C-5) of the 1-naphthol ring in both the ground and the excited states. Furthermore, the photoacidity of 1-naphthol-3,6-disulfonate, one of the first derivatives of 1-naphthol which was investigated for its ultrafast kinetics on the picosecond time-scale,<sup>65</sup> has been reinvestigated using Marcus's free-energy correlations suitable for describing charge-transfer reactions in solutions.

## 2. EXPERIMENTAL SECTION

1-Naphthol-3,6-disulfonic acid disodium salt hydrate was purchased from Aldrich and recrystallized before use. D<sub>2</sub>O (99.90%) was purchased from Deutero. 1-Naphthol-5-*tert*-butyl (1N-StBu) was synthesized in the group of Prof. Laren M. Tolbert at Georgia Tech (Atlanta) by Anne Margaret Hess Manay. 1-Naphthol-5-sulfonate (1N-SS) was purchased from TCI Japan and used as received. All solvents were of spectroscopic grade and were purchased from Aldrich.

Steady-state spectra were recorded on a JASCO 570 spectrophotometer and Cary Eclipse Varian fluorometer. Single-photon counting measurements were carried out with a setup similar to the one described before.<sup>31</sup> Time resolution of the data acquisition card was 3.14 ps per channel at the 25 ns full-scale of the apparatus. The kinetic curves were analyzed by convolution with the instrument response function (20 ps at fwhm) using Matlab software version 7.2. All fluorescence emission and infrared absorption experiments were carried out at 21 °C.

Ultrafast infrared spectra were recorded using an experimental setup described previously.<sup>33</sup> Electronic excitation was achieved with pulses (3  $\mu$ J, 50 fs) generated by sum frequency mixing of the fundamental of a 1 kHz amplified Ti:sapphire laser (Tsunami oscillator with Spitfire Pro regenerative and booster amplifier stages, Spectra Physics) and visible pulses generated by a noncollinear optical parametric amplifier (NOPA). The excitation wavelength was tuned to 334 nm corresponding to the lowest energy peak of the <sup>1</sup>L<sub>b</sub> transition thereby ensuring minimal excess energy. The pump pulses were sent to a delay line and then focused onto the sample with a beam diameter of approximately 200  $\mu$ m. Tunable mid-infrared pulses were generated by a double-pass optical parametric amplifier followed by difference frequency mixing of signal and idler. The probe and reference pulses were obtained using reflections from a ZnSe wedge and focused onto the sample by

means of an off-axis parabolic mirror (focal diameter 150  $\mu$ m). The probe and reference pulses were dispersed in a polychromator (8–10 cm<sup>−1</sup> resolution) and spectrally resolved absorbance changes were recorded simultaneously for each shot using a liquid nitrogen cooled HgCdTe double array detector (2 × 31 pixels). The time resolution was determined to be 150 fs on the basis of the cross-correlation between the UV pump and IR-probe pulses measured in a ZnSe semiconductor placed at the sample position. A peristaltic pump was used to circulate the sample through a flow cell (1 mm thick CaF<sub>2</sub> windows separated by a 25  $\mu$ m thick Teflon spacers), to guarantee that a new sample volume was excited for every laser shot. In addition, given the formation of a photoproduct sticking to the cell window, which is a well-known phenomenon in aromatic systems with electron-donating substituents, the sample holder was moved up and down during the measurement. Furthermore, the electronic and steady-state infrared spectra before and after the measurement were monitored to ensure that the nature of the solution did not change.

## 3. RESULTS

**3.1. Steady-State Measurements.** The absorption and fluorescence spectra of three derivatives of 1N photoacids were measured in H<sub>2</sub>O. In other cases where the fluorescence signal coming from the excited photoacid was too small to measure in H<sub>2</sub>O, D<sub>2</sub>O was used instead. Representative electronic absorption and emission spectra of the photoacids are given in Figure 1 for 1-naphthol-3,6-disulfonate (1N-3,6diS) and 1-naphthol-5-*tert*-butyl (1N-StBu) dissolved in H<sub>2</sub>O and 1-naphthol-5-sulfonate (1N-SS) dissolved in D<sub>2</sub>O.

Table 1 summarizes the spectroscopic and thermodynamic data used in the Förster cycle calculations of the pK<sub>a</sub>\* values of the photoacids.

**3.2. Time-Resolved Measurements.** We have measured steady-state and transient IR spectra of 1N-3,6diS in H<sub>2</sub>O and in D<sub>2</sub>O (Figure 2). Changes in vibrational mode patterns associated with aromatic ring “breathing” motion and vibrational modes of the side groups in the fingerprint region of the IR absorption spectrum in between 1000 and 1500 cm<sup>−1</sup> will occur upon electronic excitation, or even more pronouncedly when the photoacid converts into the conjugate photobase when releasing a proton to the solvent.<sup>33–46</sup> Many vibrational transitions in the fingerprint region can be observed for 1N-3,6diS in the electronic ground state of the photoacid with the most intense peaks around 1200 cm<sup>−1</sup> associated with vibrations of the sulfonate-side groups. The ESPT dynamics of 1N-3,6-diS in H<sub>2</sub>O are determined by fitting the disappearance of the broad photoacid peak around 1350 cm<sup>−1</sup> and the appearance of the narrow conjugate photobase peak at 1305 cm<sup>−1</sup> to a monoexponential function, giving a value of 5.9 ± 0.5 ps. In a similar fashion, the dynamics of 1N-3,6-diS in D<sub>2</sub>O give a 13 ± 0.5 ps characteristic time constant (Figure 3b). The proton dissociation reaction of strong photoacids may also be measured by time-resolved fluorescence techniques in aqueous solutions. Typical time-resolved dissociation profiles of a strong photoacid, 1-naphthol-5-sulfonate, (1N-SS) were measured employing the time correlated single photon counting technique (TCSPC) in water and D<sub>2</sub>O solvents (Figure 3a). Here the dynamics of 1N-SS are fitted by convoluting the exponential function with the instrument response function of the experimental setup and then best-fitting the synthetic decay curve with the measured

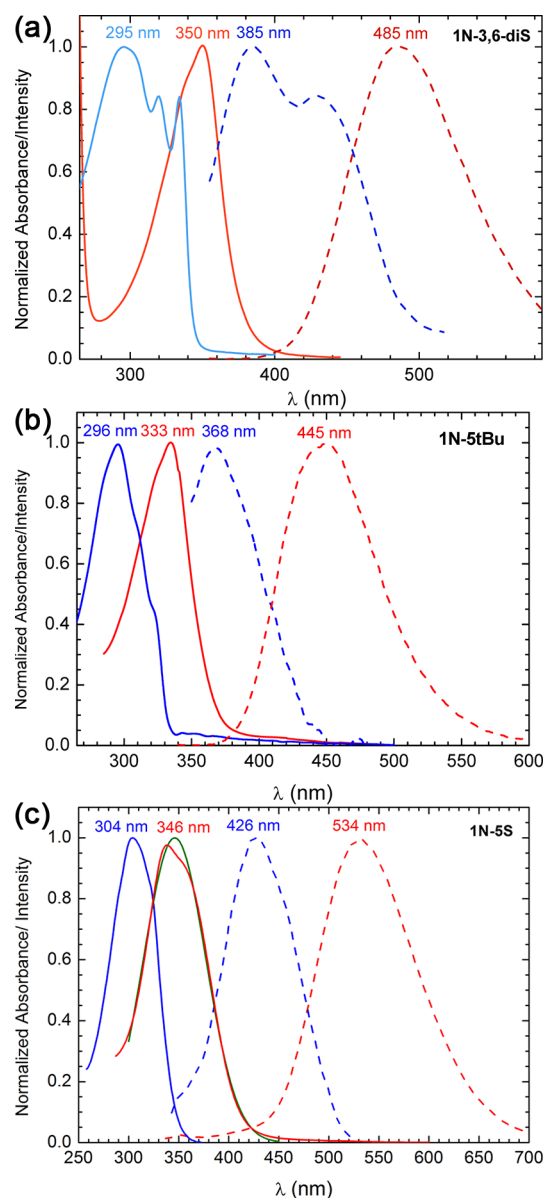


**Figure 1.** (a) Absorption (solid lines) and fluorescence (dashed lines) spectra of acid (blue) and anion (red) forms of 1N-3,6-disulfonate (1N-3,6-diS) in H<sub>2</sub>O. The excitation wavelength for the fluorescence spectra was 300 nm. The fluorescence emission of the acid form was obtained by subtracting the fluorescence spectrum at pH = 10.5 (red) from fluorescence spectrum at pH = 1. The secondary peak of the acid fluorescence at 430 nm overlaps with the anion fluorescence and was found to slightly affect the position of the apparent maximum intensity of the anion fluorescence when the spectrum of the anion is taken when it is formed indirectly following the ultrafast dissociation of the photoacid. (b) Absorption (solid lines) and fluorescence (dashed lines) spectra of acid (blue) and anion (red) forms of 1-naphthol-5-*tert*-butyl (1N-5tBu) in H<sub>2</sub>O. The fluorescence emission of the acid form was obtained by subtracting the fluorescence spectrum at pH = 11.5 (red) from the fluorescence spectrum at pH = 1. (c) Absorption (solid lines) and fluorescence (dashed lines) spectra of acid (blue) and anion (red) forms of 1-naphthol-5-sulfonate (1N-5S) in D<sub>2</sub>O. The fluorescence emission of the acid form (blue dashed line) was obtained by subtracting the fluorescence spectrum at pD = 10.7 (red dashed line) from the fluorescence spectrum at pD = 1. The maximum of the acid fluorescence at 346 nm was found by fitting of the top of fluorescence spectra to a Gaussian function (solid red line).

**Table 1.** Spectroscopic and Thermodynamic Data of Some 1-Naphthol Derivatives in Water

photoacid	absorption (nm)		fluorescence (nm)		$\Delta pK_a$	$pK_a^0$	$pK_a^*$
	acid	anion	acid	anion			
1N-3,6diS	295	350	385	485	11.2	8.6 <sup>66</sup>	−2.6
1N-5-tBu	296	333	367	443	8.8	9.8 <sup>67</sup>	+1.0
1N-5S	304	346	426	534	9.1	8.4 <sup>16</sup>	−0.7

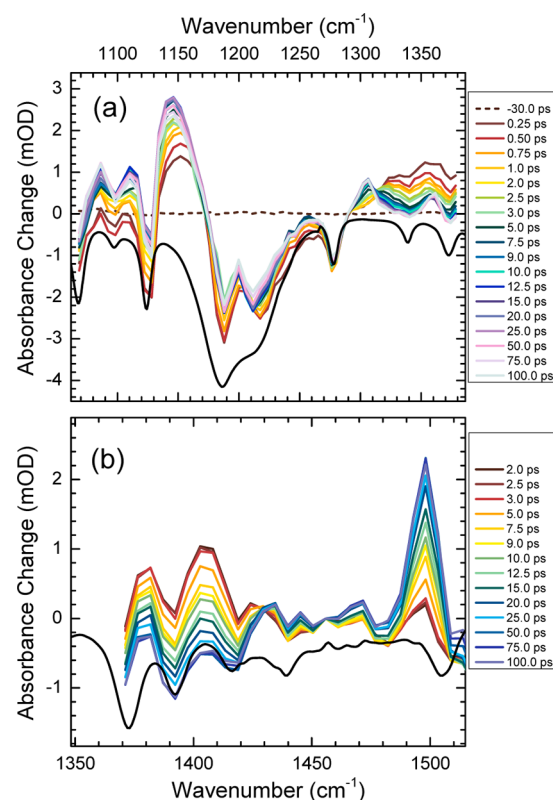


**Figure 2.** Time resolved IR spectra of 1N-3,6-disulfonate in neutral H<sub>2</sub>O and D<sub>2</sub>O. The excitation wavelength was 330 nm. The solid lines in black are the inverted ground-state spectra taken prior to optical excitation. The time elapsed between the exciting optical pulse and the IR probe pulse is color-indicated in the figure.

one.<sup>31</sup> The decay time constants thus found were  $15 \pm 3$  ps in H<sub>2</sub>O and  $32 \pm 3$  ps in D<sub>2</sub>O.

As our measurements indicate, typical proton transfer of Brønsted acids<sup>1</sup> in H<sub>2</sub>O occurs with a rate constant  $k_H$  larger than the corresponding deuterium-transfer rate  $k_D$  of the deuterated acid in D<sub>2</sub>O. The isotope effect on the proton-transfer rate constant is evidenced by the ratio  $k_H/k_D$  that has values ranging from 1.6 to 3.8 for the compounds discussed here (see Table 2 in the Discussion for values).

## 4. DISCUSSION

**4.1. Photoacidity and Förster Cycle.** The Förster Cycle<sup>8</sup> is an excellent starting point for the discussion of photoacidity, as it allows the estimation of the excited-state acidity of many photoacids from simple, readily done optical measurements, and establishes the idea that photoacids may be treated from a thermodynamic point of view similar to ordinary ground-state acids. Another method, mainly developed by Weller, is the direct titration of the fluorescence of the photoacid and the conjugated photobase.<sup>10</sup> However, the most accurate determi-



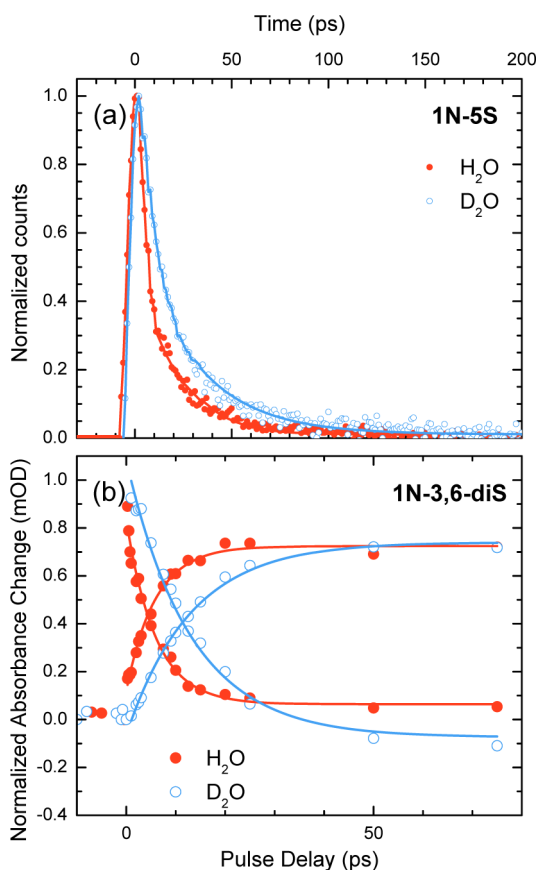


**Figure 3.** (a) Time correlated single photon counting decays of the 1N-5S photoacid measured at 425 nm in H<sub>2</sub>O (red dots) and in D<sub>2</sub>O (blue dots). The solid line is the convolution of the exponential decay with the instrument response function. The decay time constants were  $15 \pm 3$  ps in H<sub>2</sub>O and  $32 \pm 3$  ps in D<sub>2</sub>O. Excitation wavelength was 347 nm, taken at 21 °C. (b) Transient IR measurements on 1N-3,6-diS showing the decay of the photoacid marker bands and the rise of the conjugate photobase bands, depicted as dots in H<sub>2</sub>O (red) and D<sub>2</sub>O (blue). For the H<sub>2</sub>O measurements, the acid decay was measured at  $1350\text{ cm}^{-1}$  and the base rise at  $1310\text{ cm}^{-1}$ . In D<sub>2</sub>O marker bands were probed at  $1403\text{ cm}^{-1}$  (photoacid form) and at  $1498\text{ cm}^{-1}$  (conjugate photobase form). A residual electronic ground-state bleach signal at  $1403\text{ cm}^{-1}$  results in a finite negative value at long pulse delays.

nation of the  $pK_a^*$  of a photoacid in the electronically excited state is by direct kinetic measurements of the excited-state proton dissociation and recombination rates.<sup>18,19,22,23,37,68,69</sup>

Although these methods may serve to estimate the excited-state acidity of photoacids, unfortunately, no method constitutes a general method for accurate (analytic) determination of  $pK_a^*$  values. Indeed, direct kinetic measurements, developed by Pines and Huppert using time-resolved single photon counting measurements of high accuracy,<sup>22,23,68–70</sup> are limited to a small number of photoacids where the demanding task of taking precise measurements of the excited-state reversible dynamics of the proton-transfer reactions is possible.<sup>22,69</sup> Likewise, titrating the fluorescence of strong photoacids with negative  $pK_a^*$  values is not practical, as it requires solutions of highly concentrated mineral acids which then often quench the fluorescence of both the photoacid and the conjugated photobase. In addition, unintentional protonation of side groups of the photoacid and even the aromatic backbone occur in parallel to the gradual protonation of the main functional group of the photobase.<sup>3,4</sup> This common phenomenon has nonetheless never been taken into account in the  $pK_a^*$  calculations of strong photoacids because of the extreme difficulties in quantifying analytically the extent of the various surplus protonation reactions as a function of the pH. These surplus protonation reactions gradually change the overall charge of the chromophores at the low pH range needed for the titration of the photobase emission. Finally, the titration curves need to be corrected for the change in the ionic strength of the solution, a correction procedure which has seldom been performed due to its complexity and uncertainty at lower pH values due to the gradual onset of the surplus protonation reactions. These difficulties rationalize the observed large spread in the reported  $pK_a^*$  values of strong photoacids. One notable example is that of 8-hydroxypyrene-1,3,6-trisulfonate (HPTS) for which Weller reported a  $pK_a^*$  value of almost 1  $pK_a$  unit smaller than the true value that was found by Pines et al. using precise direct kinetic measurements of the excited-state geminate recombination reaction of the HPTS anion following the ESPT reaction from the photoacid to the solvent.<sup>18,19,23</sup> A second example is that of 1-naphthol whose  $pK_a^*$  value was long considered to be similar to that of 2-naphthol.<sup>11</sup> This was first corrected from the originally reported  $pK_a^*$  of about 2 to 0.4 when the effect of the ultrafast quenching reaction by protons of both the photoacid and the conjugated photobase fluorescence was taken into account.<sup>60,61,71</sup> This quenching reaction was attributed to the protonation of the aromatic ring at the C-5 and C-8 position.<sup>61</sup> Later on, the  $pK_a^*$  value of 1-naphthol was further corrected to about 0 when the two parallel geminate recombination reactions of the proton were taken

**Table 2.**  $pK_a$  and  $pK_a^*$  and Excited-State Kinetic Parameters for Various Derivatives of 1-Naphthol

	1N	1N-4S	1N-5S	1N-3,6-diS	1N-5CN	1N-5tBu
$pK_a$	9.4 <sup>73</sup>	8.3 <sup>74</sup>	8.4 <sup>16</sup>	8.6 <sup>66</sup>	8.05 <sup>31</sup>	9.8 <sup>67</sup>
$pK_a^*$	−0.2 <sup>62</sup>	−0.1 <sup>74</sup>	−0.7 <sup>a</sup>	−2.6 <sup>a</sup>	−2.8 <sup>31</sup>	1.0 <sup>a</sup>
$\tau_{H_2O}$	35 ps <sup>71</sup>	33 ps <sup>75</sup>	15 ps <sup>a</sup>	5.9 ps <sup>a</sup>	8 ps <sup>31</sup>	290 ps <sup>a</sup>
$\tau_{D_2O}$	133 ps <sup>73</sup>	110 ps <sup>76</sup>	32 ps <sup>a</sup>	13 ps <sup>a</sup>	13 ps <sup>31</sup>	1 ns <sup>a</sup>
$k_H/k_D$	3.8	3.3	2.1	2.2	1.6	3.4

<sup>a</sup>This work.

into account; one an irreversible protonation reaction leading to fluorescence quenching and the other a reversible protonation reaction leading back to the electronically excited photoacid.<sup>62–64</sup> These revisions have now placed 1-naphthol in the category of strong photoacids with a  $pK_a^*$  value of almost 3  $pK_a$  units less than that of 2-naphthol.

Considering these difficulties and uncertainties in determining the  $pK_a^*$  of 1-naphthol, we have chosen to use the Förster Cycle method to estimate the change in the  $pK_a$  value of photoacids upon optical excitation. The relation between and the observed spectral shifts may be written in a compact form using the difference in the 0–0 transition energies of the acid and base states expressed by the electronic transition frequencies  $\Delta\nu$  ( $\text{cm}^{-1}$ ), eq 1:<sup>8–10</sup>

$$\Delta pK_a = pK_a^* - pK_a = (0.625 \text{ K/T})(\Delta\nu/\text{cm}^{-1}) \quad (1)$$

The average spectral shifts in the maxima of the absorption and fluorescence spectra of the photoacid and photobase have been used in calculating  $\Delta\nu$ ;  $T$  is the absolute temperature in Kelvin.

The use of eq 1, although straightforward, also leads to large uncertainties in the determination of the  $pK_a^*$  values of strong photoacids. This is mainly due to replacing the 0–0 transition energies by the observable peak intensities of the spectra and the difficulty in accurately measuring the fluorescence spectra of the photoacid with negligible quantum yields due to its rapid dissociation. The direct approach to circumvent the latter difficulty, as in the fluorescence titration method, has been to take the spectrum of the photoacid at very low pH where proton recombination is a more efficient process than proton dissociation. However, this simple approach to increase the fluorescence signal coming from the photoacid fails when the photoacid is quenched by protons, as is the case for 1-naphthol. This experimental shortcoming adds to the systematic difficulties associated with very low pH conditions as discussed above for the case of the fluorescence titration method. Furthermore, the Stokes shifts at low pH will also depend on the solution pH because the solvating powers of the solvent and hence the solvent induced Stokes shifts of all solutes are slightly but increasingly affected in concentrated acid solutions when approaching the concentration limits of the pure-acid solutions.<sup>72</sup> For the same reason, use of organic solvents such as alcohols where ESPT does not occur to monitor the fluorescence of the photoacid leads to significant discrepancies. Indeed, photoacids in organic solvents have significantly different magnitudes for the Stokes shift compared to those in water. This renders the direct use of fluorescence spectra taken in nonaqueous solutions for the purpose of accurate Förster cycle calculations highly questionable.

To circumvent the need for a very acidic environment to detect the photoacid emission, we have taken the fluorescence spectra of 1N-SS in  $D_2O$ . The advantage being that  $D_2O$  solutions have negligible differences in Stokes shift compared to  $H_2O$  solutions, yet reduce the proton-transfer rate to the solvent thereby increasing the emission from the undissociated photoacid by a factor of 2–3. The spectra have been taken at above  $pD = 1$ , which is a  $pD$  not low enough to cause any of the complications discussed above but acidic enough so the emission coming from the undissociated photoacid is increased by favorable proton recombination conditions. Even under such conditions, the fluorescence intensity of the photoacid was still only a few percent of the emission intensity of the photobase. It was thus necessary to precisely subtract the fluorescence profile

of the anion from that of the acid to recover the pure fluorescence spectra of the photoacid (Figure 1c).

Finally, we have taken the location of the peak of the spectra from fitting the top of the spectral curves to a Gaussian function; see Figure 1c for one visual example of the fitting procedure. This procedure has generally led to better correspondence between the  $pK_a^*$  calculated from the absorption spectra with the one calculated from the emission spectra of the photoacid.

Using the above-described procedures, we have found  $pK_a^*$  values (–2.6 for 1N-3,6diS and –0.7 for 1N-SS) that were more acidic than the ones available in the literature (1.1 for 1N-3,6diS<sup>16</sup> and 0.04 for 1N-SS,<sup>65</sup> the reported value for 1N-3,6diS being a typo and should have been –1.1) (Table 2).

The  $pK_a^*$  values were compared with the ESPT rates found for the same photoacids. This correlation of  $pK_a$  values with the reactivity of the acids was originally initiated by Brønsted in the so-called Brønsted correlation analysis.<sup>1,2</sup> We have used two modern-day free-energy procedures to correlate our kinetic data with our thermodynamic data. The C-5 position was singled out because it is one of the most reactive positions on the aromatic ring of the naphthalene system. The C-5 position is also the position where protonation of the aromatic ring was suggested to cause the deactivation of the naphtholic system.<sup>3,4,61</sup> For that purpose, we have also studied the photoacidity of the 1N-5tBu derivative of 1-naphthol which was found by the Tolbert group<sup>77</sup> to lose the *tert*-butyl group in the excited electronic state by an exchange reaction with  $H^+$ .

**4.2. Free-Energy–Reactivity Correlation.** Most modern theories that rationalize the empiric Brønsted correlation of acid reactivity treat proton transfer in aqueous solution as a dynamic process closely coupled with solvent motion and solvent relaxation.<sup>78–96</sup> They assume that the proton-transfer rate between a proton donor and a proton acceptor  $k_d$  has a general form akin to a transition-state rate constant that may be written as

$$k_d = \frac{w}{2\pi} \exp\left(-\frac{\Delta G^\ddagger}{RT}\right) \quad (2)$$

where  $R$  is the gas constant,  $T$  is the absolute temperature,  $w$  is the frequency factor of the proton-transfer reaction, which may also depend on solvent relaxation frequencies, and  $\Delta G^\ddagger$  is the effective activation energy of the proton-transfer reaction in the excited state that may be estimated using Marcus reaction model originally developed for outer-sphere (nonadiabatic) electron-transfer reactions.<sup>82–85</sup> According to the Marcus theory for electron transfer, charge-transfer reactions proceed along the solvent coordinate with an intrinsic activation energy equal to one-fourth of the total solvent reorganization energy for a hypothetical vertical charge-transfer reaction when the solvent coordinate is frozen while the reaction takes place.<sup>82–85</sup> The potential energy of such a two-state reaction model having reactant- and product-energy wells is represented by a pair of intersecting parabolas with their intersection point giving the activation energy needed for the transfer from the reactant to the product state:

$$\Delta G^\ddagger = \left(1 + \frac{\Delta G^0}{4\Delta G_0}\right)^2 \Delta G_0 \quad (3)$$

where  $\Delta G_0^\ddagger$  is the intrinsic activation energy of a symmetric transfer where the total free-energy change ( $\Delta G^0$ ) following the charge transfer is equal to zero.

An important aspect of Marcus Theory when applied semiempirically to proton-transfer reactions,<sup>15,21,31–33,44</sup> is the direct correspondence between the acidity constant of the acid,  $pK_a$ , and the correlating factor of a family of similar proton-transfer reactions  $\Delta G^0$ :

$$\Delta G^0 = RT \ln(10)pK_a \quad (4)$$

Marcus theory gives a central role to solvent reorganization in charge-transfer reactions in polar solvents where solvent reorganization energy is large.<sup>82–85</sup> Marcus, and subsequently Marcus and Cohen, modified the electron-transfer theory (ET theory) suitable for two very weakly interacting potential wells of a reactive system and applied it in a semiempiric way to proton-transfer reactions by using a bond-energy-bond-order (BEBO) model for the proton-transfer coordinate along a pre-existing hydrogen-bond.<sup>97</sup> The semiempiric BEBO treatment represents the opposite extreme condition to nonadiabatic electron-transfer reactions. In the BEBO model, bond rupture and bond formation is the principal contributor to the reaction coordinate.<sup>97</sup> In this case, the potential energy along the reaction coordinate is initially constant and then rises to a maximum at the transition state after which it falls to another constant value. The activation energy is given by

$$\Delta G^\ddagger = \frac{\Delta G^0}{2} + \Delta G_0^\ddagger + \frac{\Delta G_0^\ddagger}{\ln 2} \ln \left( \cosh \left( \frac{\Delta G^0 \ln 2}{2\Delta G_0^\ddagger} \right) \right) \quad (5)$$

Remarkably, the two seemingly different approaches (i.e., eqs 3 and 5) yield almost identical results in the endothermic branch of the reactions. This also corresponds to our observation window in the free-energy correlation portrayed in Figure 4. Evidently, at the extreme exothermic branch of the free-energy correlation, the approaches differ considerably but this branch was not accessed in our present set of photoacids.

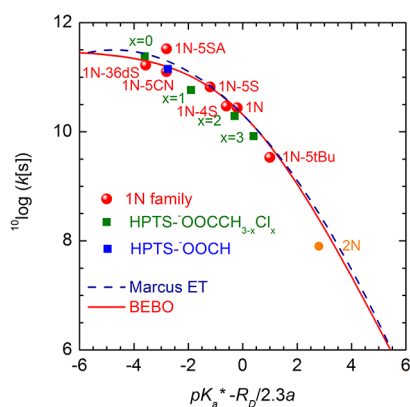


**Figure 4.** Free-energy correlation found in the proton dissociation reaction of 1-naphthol derivatives (Table 2) the 5-sulfamide substituent of 1-naphthol (1N-5SA)<sup>67</sup> and also 2-naphthol (2N). Also shown in the correlation the kinetic rate constants for the direct proton-transfer reaction between photoacids and carboxylate bases.<sup>44</sup> All reaction rates were taken at room temperature (dots). The dashed line is for the Marcus ET correlation, eq 3 and the solid line is for the Marcus BEBO equation, eq 5. The parameters of the fits are  $\log(k_0) = 11.5$  for the activationless proton-transfer rate and,  $\Delta G_0^\ddagger = 1.6$  kcal for the intrinsic barrier common for all the proton-transfer reactions.

Though Marcus theory predicts an “inverted region” where, due to the quadratic nature of eq 3, activation energy “reappears” when the driving force of the reaction becomes very large, it is not so with the BEBO model, eq 5, where the reaction rate assumes a constant (maximal) value in this limit. Constructing a full experimental Marcus plot for proton transfer from a set of structurally related Brønsted acids extending all the way to the zone of the Inverted Region of the reaction has remained one of the most alluring challenges in proton-transfer research.

In the past years we have conducted comparative femto-second infrared studies of the bimolecular proton-transfer reaction dynamics of the photoacid 8-hydroxypyrene-1,3,6-trisulfonate (HPTS) with a series of carboxylate bases  $^-OOCCH_3$  and  $^-OOCCH_2(3-x)Cl_x$  ( $x = 0–3$ ) in aqueous solution.<sup>33–36,38–41,43</sup> We have also followed dynamics of the proton transfer from 2-naphthol-6,8-disulfonate (2N-6,8diS) to bicarbonate by inspection of appropriate vibrational modes marking the progress of the reaction. We have routinely correlated the measured rates of on-contact proton-transfer reactions with the free-energy change accompanying these on-contact reactions, either by using the functional form of the free-energy correlation as predicted by the Marcus ET theory, or alternatively by using the Marcus–Cohen BEBO approach for proton-transfer reactions.<sup>33,44</sup> Although, as already discussed above, the two approaches represent two completely different reactive conditions, they result in an almost identical dependence of the proton-transfer rate on the  $\Delta pK_a$  in the reactivity range probed by our experiments. The functional resemblance between adiabatic and nonadiabatic proton-transfer reactions over a limited range of reactivity was theoretically rationalized by Kiefer and Hynes.<sup>90–96</sup> In the Kiefer and Hynes theory, proton nuclear motion was treated quantum mechanically but the proton did not tunnel as the reaction barrier was found to fluctuate because of solvent rearrangements to below the zero-point energy of the proton. This description of nonadiabatic proton transfer strongly differs from Marcus semiempiric BEBO treatment in the quantization of the proton and considering the solvent coordinate as the reaction coordinate. Remarkably, despite the different treatment, Kiefer and Hynes showed that the reaction path of the proton transfer characterized by the values of the quantum-averaged proton coordinate is very similar to the BEBO pathway and by doing so have justified the use of the readily applied BEBO model as one of the most important semiempiric tools for correlating the reactivity of families of structurally related acids.<sup>90,91</sup>

In Figure 4 we depict the free-energy reactivity correlation, together with experimental results on 1-naphthol photoacid derivatives in aqueous solution as presented in Table 2, as well as from aqueous proton transfer between HPTS and carboxylate bases.<sup>33–36,38–41,43</sup> Also included is the data point for the proton dissociation of the 2-naphthol photoacid in water. The  $pK_a$  values of the variously charged photoacids were adjusted to reflect the free-energy change at contact separation of singly charged ions as required when the Marcus equation is used to correlate a family of reactions involving various charges. Such a procedure takes into account the thermodynamic definition of dissociation constants which includes the extra work (free energy) needed to separate oppositely charged reaction products to infinite separation.<sup>3,4</sup> In Figure 4  $R_D$  is the Debye radius,  $R_D = q_1q_2$  and  $a$  is the contact radius.<sup>38</sup> Similarly to our past observations, the experimental data could be equally well correlated by both the ET and BEBO expressions for the



proton transfer, as the proton-transfer reactions of these strong photoacids are still in the “normal” region of the Marcus ET theory. The free-energy correlation plots as such shows that all photoacids studied here behave in a normal fashion; i.e., the substituent affects the  $pK_a^*$  of the naphtholic system by its electron-donating or accepting abilities, which are scaled according to the particular position that the substituent occupies on the aromatic ring system and the Hammett  $\sigma$  value of the substituent.

Judging by Figure 4, the  $pK_a^*$  values of the 1-naphthol family nicely correlates with the corresponding ESPT rates. This observation is also true for 1N-5tBu photoacid, where in addition to the increased Brønsted acidity, the aromatic ring has been shown to participate in an exchange reaction with  $H^+$  replacing the *tert*-butyl group.<sup>77</sup> This observation supports the previous observation that the quenching reaction of 1-naphthol runs parallel to, and does not affect the proton dissociation reaction from the OH group.

Another aspect of the good correlation shown in Figure 4 concerns the nature of the emitting state of 1-naphthol. Clearly, the set of ESPT reactions seems regular and in line with the general free-energy correlations found for solvent assisted proton-transfer reactions of hydroxyarenes photoacids in aqueous solutions.<sup>15,30,33</sup> To verify that the behavior of the reaction set of the 1-naphthol family is indeed regular and in line with the general substituent effect observed for aromatic systems in the ground state, we have plotted the Hammett  $\sigma$  values of the substituents against the equilibrium constant values of the photoacids in the ground and the excited state in Figure 5. The first conclusion that may be drawn is that ring-

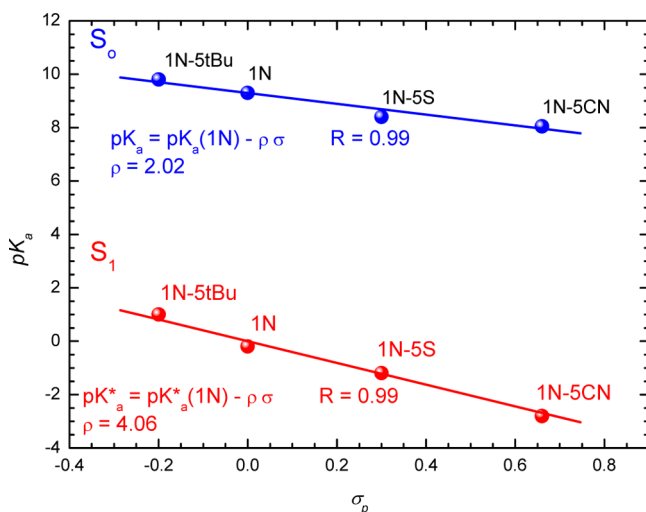


**Figure 5.**  $pK_a^0$  and  $pK_a^*$  values vs Hammett's  $\sigma$  values for 1-naphthol substituents at the C5 position. The  $\rho$  and  $R$  values of the correlations are indicated in the figure.

substituents at the 5-position of the 1-naphthol ring cause a change in the same direction for both the  $K_a$  and  $K_a^*$ , with the substituents having a greater substituent effect in the electronic excited state of the photoacid. It follows that one may discuss the effect of various types of substituents on photoacidity using arguments and terminology that have been traditionally used for ground-state acids. A similar conclusion may be drawn from similar analysis taken on 1-naphthol derivatives at other ring positions.<sup>3,4</sup> In particular, using the vast body of work of Hammett<sup>98</sup> and Taft,<sup>99,100,101</sup> one can conclude that their

structure–reactivity arguments are also valid for the excited state of aromatic acids albeit with different scaling factors than in the ground state; i.e., they have different  $\rho$  values in the Hammett equation.<sup>5</sup> For the 1-naphthol family of the 5-C substituents, we have found a  $\rho$  value for the ESPT equilibrium constant twice as large as the  $\rho$  value found in the ground electronic state of the same set of photoacids (Figure 5).

Finally, the observed net effect in the change in photoacidity for one substituent on either increasing or decreasing photoacidity is less than 3  $pK_a^*$  units in even the most extreme cases studied so far.<sup>5,102</sup> As this only constitutes about one-third of the total acidity change upon electronic excitation, it thus appears that in most cases it is valid to treat the substituent effect as a perturbation to the electronic structure of the unsubstituted chromophore, even when the aromatic acid is in the electronic excited state.<sup>102</sup>

Taking a closer look at the substituent effect at the C5 position, it was indeed found to lead to one of the largest substituent effects on the 1-naphthol ring.<sup>3,4</sup> The sulfonate and cyano groups enhance charge transfer from the oxygen atom to the aromatic system (Hammett  $\sigma_p$  values = 0.36 and 0.66, respectively, taken from the benzoic acid analogs<sup>101</sup>). The situation is reversed with the bulky electron-withdrawing *tert*-butyl-group ( $\sigma_p = -0.20$ ).<sup>101</sup> It follows that 1N-5S is a much stronger photoacid mainly because it is a much stronger acid already in the electronic ground state,  $pK_a = 8.4$  compared to 1N-5tBu that has a ground-state  $pK_a = 9.8$ .

**4.3. Kinetic Isotope Effect.** We have analyzed the kinetic isotope effect (KIE) observed for the ESPT reactions of these photoacid compounds. The correlation is in fact a consequence of the general free-energy correlation including some additional assumptions needed to compare between  $H^+$  and  $D^+$  transfers. To this end, we follow the classic treatment of the KIE although it has been realized that such treatments do not capture the full complexity of this phenomenon (see below). It was first suggested by Westheimer<sup>103</sup> and Melander to correlate KIE with the free-energy change in reaction. They have argued that the KIE, as defined by  $k_H/k_D$ , will have a maximum value for a symmetrical transition state ( $\Delta G^\ddagger = 0$ ), i.e., when

$$\frac{k_H}{k_D} = \exp(-(\Delta G_H^\ddagger - \Delta G_D^\ddagger)/RT) \quad (6)$$

Such a correlation, spanning over a range of 25  $pK_a$  units, was shown by Bell in his book to hold for an extended family of carbon acids.<sup>104</sup>

Marcus, while assuming that  $\Delta G^\ddagger_0$  is the only isotope dependent quantity in eqs 3–5, derived a relationship between  $\ln(k_H/k_D)$  and the free-energy change of the proton transfer. Assuming  $(\Delta G^\ddagger_0)^2 = \Delta G^\ddagger_{0H} \Delta G^\ddagger_{0D}$  for the symmetric reaction, eq 3 gives

$$\begin{aligned} \ln\left(\frac{k_H}{k_D}\right) &\cong \left(\frac{\Delta G^\ddagger_{0H} - \Delta G^\ddagger_{0D}}{RT}\right) \left(1 - \left(\frac{\Delta G^\circ}{4\Delta G^\ddagger_0}\right)^2\right) \\ &= \left(\ln\left(\frac{k_H}{k_D}\right)\right)_{\max} \left(1 - \left(\frac{\Delta G^\circ}{4\Delta G^\ddagger_0}\right)^2\right) \end{aligned} \quad (7)$$

Equation 7 has a very simple and practically appealing form and as such is often used as a semiempiric expression. The KIE may also be estimated from the BEBO equation (eq 5), and the resulting functional BEBO form for the KIE is given by

$$\begin{aligned}
 \ln\left(\frac{k_{\text{H}}}{k_{\text{D}}}\right) &\cong \left(\frac{\Delta G_{0\text{H}}^{\#} - \Delta G_{0\text{D}}^{\#}}{RT}\right) \\
 &\times \left(1 - \frac{\frac{\Delta G^{\circ} \ln 2}{2\Delta G_0^{\#}} \tanh\left(\frac{\Delta G^{\circ} \ln 2}{2\Delta G_0^{\#}}\right) - \ln\left(\cosh\left(\frac{\Delta G^{\circ} \ln 2}{2\Delta G_0^{\#}}\right)\right)}{\ln 2}\right) \\
 &= \left(\ln\left(\frac{k_{\text{H}}}{k_{\text{D}}}\right)\right)_{\text{max}} \\
 &\times \left(1 - \frac{\frac{\Delta G^{\circ} \ln 2}{2\Delta G_0^{\#}} \tanh\left(\frac{\Delta G^{\circ} \ln 2}{2\Delta G_0^{\#}}\right) - \ln\left(\cosh\left(\frac{\Delta G^{\circ} \ln 2}{2\Delta G_0^{\#}}\right)\right)}{\ln 2}\right)
 \end{aligned}
 \quad (8)$$

The dependence of the KIE on the  $\text{p}K_{\text{a}}$  values of a family of similarly structured acids is predicted by both eqs 7 and 8 to be bell-shaped and symmetric about a maximum KIE value found at  $\text{p}K_{\text{a}} = 0$ . Both expressions, although greatly different in their physical modeling of the proton-transfer reaction, give a similar numeric dependence of the KIE on the exothermicity of the reaction in the reactivity range probed in our experiments (Figure 6).

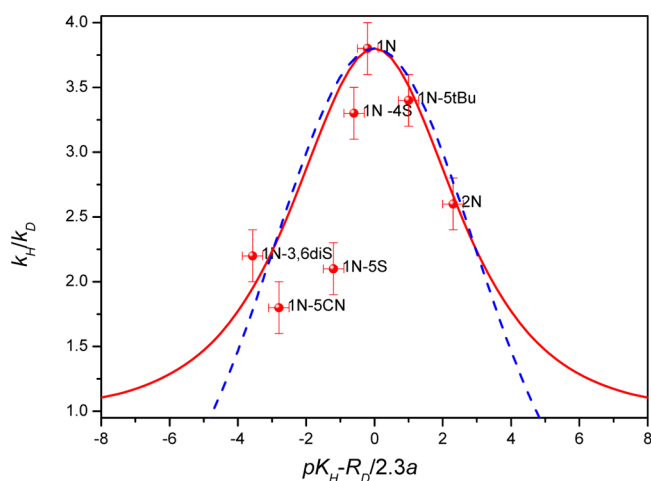


**Figure 6.** Kinetic isotope effect (KIE) as a function of the  $\text{p}K_{\text{a}}^*$  of substituted 1N and of 2 naphthol. The dashed line is the Marcus ET correlation, eq 7 and the solid line is the Marcus BEBO equation, eq 8. The parameters of the fits are  $\Delta G_0^{\#} = 1.6$  kcal and  $\ln(k_{\text{H}}/k_{\text{D}})_{\text{max}} = 3.83$ .

Recently developed ab initio theory of proton-transfer reactions undertaken by Kiefer and Hynes has resulted in a functional form similar to bell shape to the one predicted by eqs 7 and 8 and graphically shown in Figure 6, and has helped to rationalize the practical use of the semiempiric Marcus treatment of the KIE in proton-transfer reactions.<sup>94</sup>

The KIE of photoacids was reviewed by Formosinho, Arnaut, and Barroso<sup>105</sup> and by Pines.<sup>106</sup> The limited available data on the KIE of photoacids should be analyzed with some caution. The fluorescence decay rate of the excited state in the absence of proton transfer is usually 1–10 ns and is isotope dependent. In the case of the strong photoacids, the dissociation rate is much faster than its fluorescence decay and the proton-

dissociation rate on contact can be directly measured in aqueous solutions because the back-protonation reaction of the photobase by geminate recombination<sup>22,23,68–70</sup> is small and has even a smaller effect on the observed initial proton dissociation rate. Typical time-resolved dissociation profiles of strong photoacids (1N-SS and 1N-2,3diS) in water and  $\text{D}_2\text{O}$  are shown in Figure 3. For photoacids having  $\text{p}K_{\text{a}}^* > 2$ , the dissociation rates of the phenol-type photoacids become smaller than the rate of the fluorescence decay. This limits the observation range of photoacid dissociation to relatively strong photoacids. In addition, proton back-recombination is expected to have a large effect on the observed proton dissociation rate of weak photoacids, making the observed rate appear slower than the actual one.<sup>22,23,68–70</sup> To the best of our knowledge, the weakest photoacid for which the KIE has been accurately reported was 2-naphthol, having a  $\text{p}K_{\text{a}}^*$  of 2.7 in  $\text{H}_2\text{O}$  and KIE of 2.6.<sup>107</sup> This data point reliably represents the endothermic branch of the KIE free-energy plot of phenol-like photoacids. For that reason we have added 2-naphthol to our KIE correlation of the 1-naphthol photoacids (Figure 6).

Finally, to achieve H to D substitution of protic hydrogen atoms, one also needs to change the solvent. In this case substituting  $\text{H}_2\text{O}$  for  $\text{D}_2\text{O}$  is expected to increase the observed isotope effect by affecting the solvent rearrangement rate which accompanies and controls the proton-transfer reaction. However, the solvent does not affect the symmetry of the functional form of the KIE and the general bell-shaped behavior of the KIE about its maximum.

We find the experimental isotope effect of 1N photoacids to have a maximum at about  $\text{p}K_{\text{a}}^* = 0$ , which is the theoretically expected location of  $(\text{KIE})_{\text{max}}$  where it has a value of 3.8. The stronger photoacids of the 1-naphthol family with negative  $\text{p}K_{\text{a}}^*$ s exhibit much smaller KIE's down to about 1.6. This confirms the prediction that the KIE should drop sharply as a function of increased photoacidity because the intrinsic activation energy for the proton dissociation from strong photoacids is very small (Figure 6). Finally, we find the 1-naphthol family of photoacids to correlate with each other and also to correlate with other photoacids. This gives a strong indication that the family of 1-naphthol photoacids should be treated as ordinary photoacids with the proton-transfer rate mainly controlled by activation in the O–H bond and in the solvent,<sup>78–81</sup> and not as much by solvent induced intramolecular charge-transfer reaction in the aromatic residue of the photoacid.<sup>27,28</sup>

Finally, we have limited our treatment to a semiempiric description due to the inherent complexity of the systems in question, which combines proton transfer in aqueous solutions with the complex intramolecular photophysics of the 1-naphthol family of photoacids.<sup>62–64</sup>

A more robust approach to elucidating the reactive behavior of these systems should include reliable electronic structure calculations for the photoacids in the excited electronic state coupled with state of the art ab initio calculations for the proton-transfer reaction to water such as achieved by using combined QM/MM techniques.<sup>108</sup>

#### 4. CONCLUSION

On the basis of our ultrafast experiments on 1N-SS, 1N-5tBu, and 1N-3,6diS, and utilizing reported data on 1N-4S, 1N-5CN, and the parent molecule 1N, we have come to an understanding that a Marcus-type free-energy-reactivity correlation for excited-state proton transfer (ESPT) in aqueous solution



can be drawn. This approach also explains the magnitude of the kinetic isotope effect observed in aqueous ESPT reactions of these families of photoacid molecules. Our results suggest that the current approach taken should be utilized in other types of photoacids, to expand our understanding of the photoacidity phenomenon.

## AUTHOR INFORMATION

### Corresponding Author

\*E-mail: ET.J.N., nibberin@mbi-berlin.de; E.P., epines@bgu.ac.il.

### Notes

The authors declare no competing financial interest.

## ACKNOWLEDGMENTS

This paper is dedicated to Paul F. Barbara who contributed much to our current understanding of ultrafast electron and proton transfer in solution. We acknowledge the synthesis of 1N-StBu by Anne Margaret Hess Manay from Prof. Laren M. Tolbert group in Georgia Tech (Atlanta). E.P. acknowledges the support from James Franck German-Israel Binational Program in Laser-Matter Interaction and Grant No. 2006276 from the United States-Israel Binational Science Foundation (BSF). E.T.J.N. acknowledges support by the Deutsche Forschungsgemeinschaft (DFG NI 492/11.1). M.P.S. acknowledges support of her Ph.D. by the FQRNT (Fonds de recherche Québec-Nature et technologies).

## REFERENCES

- Brønsted, J. N. *Chem. Rev. (Washington, DC, U. S.)* **1928**, *5*, 231–338.
- Brønsted, J. N. *Rec. Trav. Chim. Pays-Bas* **1923**, *42*, 718–728.
- Tolbert, L. M.; Haubrich, J. E. *J. Am. Chem. Soc.* **1990**, *112*, 8163–8165.
- Tolbert, L. M.; Haubrich, J. E. *J. Am. Chem. Soc.* **1994**, *116*, 10593–10600.
- Tolbert, L. M.; Solntsev, K. M. *Acc. Chem. Res.* **2002**, *35*, 19–27.
- Weber, K. Z. *Phys. Chem.* **1931**, *15*, 18–44.
- Terenin, A.; Kariakin, A. *Nature* **1947**, *159*, 881.
- Förster, T. Z. *Electrochem* **1950**, *54*, 42–46.
- Förster, T. *Die Naturwissenschaften* **1949**, *36*, 186–187.
- Weller, A. *Prog. React. Kinet.* **1961**, *1*, 187–213.
- Ireland, J. F.; Wyatt, P. A. H. *Adv. Phys. Org. Chem.* **1976**, *12*, 131–221.
- Shizuka, H. *Acc. Chem. Res.* **1985**, *18*, 141–147.
- Arnaut, L. G.; Formosinho, S. J. J. *Photochem. Photobiol., A* **1993**, *75*, 21–48.
- Solntsev, K. M.; Tolbert, L. M.; Cohen, B.; Huppert, D.; Hayashi, Y.; Feldman, Y. *J. Am. Chem. Soc.* **2002**, *124*, 9046–9047.
- Pines, E.; Pines, D. In *Ultrafast hydrogen bonding dynamics and proton transfer processes in the condensed phase*; Elsaesser, T.; Bakker, H. J., Eds.; Kluwer Academic Publishers: Dordrecht, The Netherlands, 2003; Vol. 23, pp 155–184.
- Pines, D.; Pines, E. In *Hydrogen-Transfer Reactions*; Hynes, J. T., Klinman, J. P., Limbach, H.-H., Schowen, R. L., Eds.; Wiley-VCH: Weinheim, 2007; Vol. 1 Physical and Chemical Aspects I-III, pp 377–415.
- Huppert, D.; Pines, E. *J. Photochem.* **1981**, *17*, 134–134.
- Pines, E.; Huppert, D.; Agmon, N. *J. Chem. Phys.* **1988**, *88*, 5620–5630.
- Agmon, N.; Pines, E.; Huppert, D. *J. Chem. Phys.* **1988**, *88*, 5631–5638.
- Pines, E.; Huppert, D. *J. Am. Chem. Soc.* **1989**, *111*, 4096–4097.
- Pines, E.; Manes, B. Z.; Lang, M. J.; Fleming, G. R. *Chem. Phys. Lett.* **1997**, *281*, 413–420.
- Pines, E.; Huppert, D. *J. Chem. Phys.* **1986**, *84*, 3576–7.
- Pines, D.; Pines, E. *J. Chem. Phys.* **2001**, *115*, 951–3.
- Genosar, L.; Cohen, B.; Huppert, D. *J. Phys. Chem. A* **2000**, *104*, 6689–6698.
- Goldberg, S. Y.; Pines, E.; Huppert, D. *Chem. Phys. Lett.* **1992**, *192*, 77–81.
- Leiderman, P.; Genosar, L.; Huppert, D. *J. Phys. Chem. A* **2005**, *109*, S965–S977.
- Tran-Thi, T. H.; Gustavsson, T.; Prayer, C.; Pommeret, S.; Hynes, J. T. *Chem. Phys. Lett.* **2000**, *329*, 421–30.
- Tran-Thi, T.-H.; Prayer, C.; Millié, P.; Uznanski, P.; Hynes, J. T. *J. Phys. Chem. A* **2002**, *106*, 2244–2255.
- Pines, E.; Fleming, G. R. *J. Phys. Chem.* **1991**, *95*, 10448–10457.
- Pines, E.; Magnes, B. Z.; Lang, M. J.; Fleming, G. R. *Chem. Phys. Lett.* **1997**, *281*, 413–20.
- Pines, E.; Pines, D.; Barak, T.; Magnes, B. Z.; Tolbert, L. M.; Haubrich, J. E. *Ber. Bunsen-Ges. Phys. Chem.* **1998**, *102*, 511–517.
- Munitz, N.; Avital, Y.; Pines, D.; Nibbering, E. T. J.; Pines, E. *Isr. J. Chem.* **2009**, *49*, 261–272.
- Adamczyk, K.; Prémont-Schwarz, M.; Pines, D.; Pines, E.; Nibbering, E. T. J. *Science* **2009**, *326*, 1690–1694.
- Rini, M.; Magnes, B.-Z.; Pines, E.; Nibbering, E. T. J. *Science* **2003**, *301*, 349–352.
- Mohammed, O. F.; Pines, D.; Nibbering, E. T. J.; Pines, E. *Angew. Chem., Int. Ed.* **2007**, *46*, 1458–1461.
- Mohammed, O. F.; Pines, D.; Dreyer, E.; Pines, E.; Nibbering, E. T. J. *Science* **2005**, *310*, 83–86.
- Pines, D.; Nibbering, E. T. J.; Pines, E. *J. Phys. Condens. Matter* **2007**, *19*, 065134.
- Rini, M.; Pines, D.; Magnes, B. Z.; Pines, E.; Nibbering, E. T. J. *J. Chem. Phys.* **2004**, *121*, 9593–9610.
- Nibbering, E. T. J.; Fidler, H.; Pines, E. *Annu. Rev. Phys. Chem.* **2005**, *56*, 337–367.
- Nibbering, E. T. J.; Pines, E. In *Hydrogen-Transfer Reactions*; Hynes, J. T., Klinman, J. P., Limbach, H.-H., Schowen, R. L., Eds.; Wiley-VCH: Weinheim, 2007; Vol. 2 Physical and Chemical Aspects IV-VII, pp 443–458.
- Mohammed, O. F.; Dreyer, J.; Magnes, B.-Z.; Pines, E.; Nibbering, E. T. J. *ChemPhysChem* **2005**, *6*, 625–636.
- Adamczyk, K.; Varma, S.; Ghosh, H. N.; Pines, E.; Nibbering, E. T. J. On the Transient Broadband Absorption Observed in Femtosecond Infrared Spectroscopy of Photoacids in Solution, in preparation.
- Adamczyk, K.; Dreyer, J.; Pines, D.; Pines, E.; Nibbering, E. T. J. *Isr. J. Chem.* **2009**, *49*, 217–225.
- Mohammed, O. F.; Pines, D.; Pines, E.; Nibbering, E. T. J. *Chem. Phys.* **2007**, *341*, 240–257.
- Mohammed, O. F.; Pines, D.; Dreyer, J.; Pines, E.; Nibbering, E. T. J. In *Ultrafast Phenomena XV*; Corkum, P., Jonas, D., Miller, R. J. D., Weiner, A. M., Eds.; Springer Ser. Chem. Phys. 88; Springer, Berlin, 2007; pp 412–414.
- Mohammed, O. F.; Adamczyk, K.; Pines, D.; Pines, E.; Nibbering, E. T. J. In *Ultrafast Phenomena XVI*; Corkum, P., De Silvestri, S., Nelson, K. A., Riedle, E., Schoenlein, R., Eds.; Springer Ser. Chem. Phys. 92, Springer, Berlin, 2009; pp 622–624.
- Siwick, B. J.; Cox, M. J.; Bakker, H. J. *J. Phys. Chem. B* **2008**, *112*, 378–389.
- Siwick, B. J.; Bakker, H. J. *J. Am. Chem. Soc.* **2007**, *129*, 13412–13420.
- Cox, M. J.; Bakker, H. J. *J. Chem. Phys.* **2008**, *128*, 174501.
- Strandjord, A. J. G.; Courtney, S. H.; Friedrich, D. M.; Barbara, P. F. *J. Phys. Chem.* **1983**, *87*, 1125–1133.
- Strandjord, A. J. G.; Barbara, P. F. *J. Phys. Chem.* **1985**, *89*, 2355–2361.
- Strandjord, A. J. G.; Smith, D. E.; Barbara, P. F. *J. Phys. Chem.* **1985**, *89*, 2362–2366.
- Barbara, P. F.; Walsh, P. K.; Brus, L. E. *J. Phys. Chem.* **1989**, *93*, 29–34.
- Eigen, M.; Demaeyer, L. *Proc. R. Soc. London Ser. A* **1958**, *247*, 505–533.

- (55) Eigen, M.; Kruse, W.; Maass, G.; DeMaeyer, L. *Prog. React. Kinet.* **1964**, *2*, 285–318.
- (56) Weller, A. *Discuss. Faraday Soc.* **1959**, *27*, 28–33.
- (57) Weller, A. *Z. Elektrochem.* **1952**, *56*, 662.
- (58) Hynes, J. T.; Tran-Thi, T. H.; Granucci, G. *J. Photochem. Photobiol. A: Chem.* **2002**, *154*, 3–11.
- (59) Rosenberg, J. L.; Brinn, I. *J. Phys. Chem.* **1972**, *76*, 3558–3562.
- (60) Harris, C. M.; Selinger, B. M. *J. Phys. Chem. A* **1980**, *84*, 1366.
- (61) Webb, S. P.; Philips, L. A.; Yeh, S. W.; Tolbert, L. M.; Clark, J. H. *J. Phys. Chem.* **1986**, *90*, 5154–5164.
- (62) Pines, E.; Fleming, G. R. *Chem. Phys.* **1994**, *183*, 393–402.
- (63) Pines, E.; Tepper, D.; Magnes, B. Z.; Pines, D.; Barak, T. *Ber. Bunsen-Ges. Phys. Chem.* **1998**, *102*, 504–510.
- (64) Pines, E.; Magnes, B. Z.; Barak, T. *J. Phys. Chem. A* **2001**, *105*, 9674–9680.
- (65) Masad, A.; Huppert, D. *J. Phys. Chem.* **1992**, *96*, 7324–7328.
- (66) *Dictionary of Organic Compounds*; Chapman and Hall: New York, 1982.
- (67) Barak, T. *Ph.D. Thesis*, Ben-Gurion University of the Negev, 2005.
- (68) Pines, E.; Huppert, D.; Agmon, N. *J. Chem. Phys.* **1988**, *88*, 5620–30.
- (69) Pines, E. Private communication.
- (70) Pines, E.; Huppert, D. *Chem. Phys. Lett.* **1986**, *126*, 88–91.
- (71) Lee, J.; Robinson, G. W.; Webb, S. P.; Philips, L. A.; Clark, J. H. *J. Am. Chem. Soc.* **1986**, *108*, 6538–6542.
- (72) Pines, E. *Ph.D. Thesis*, Tel-Aviv University, 1989.
- (73) Bryson, A.; Matthews, R. W. *Aust. J. Chem.* **1963**, *16*, 401.
- (74) Henson, R. M. C.; Wyatt, A. H. *J. Chem. Soc., Faraday Trans.* **1974**, *271*, 669.
- (75) Uritski, A.; Presiado, I.; Erez, Y.; Gepshtein, R.; Huppert, D. *J. Phys. Chem. C* **2009**, *113*, 7342–7354.
- (76) Bakker, H. J.; Cox, M. J. *J. Phys. Chem. A* **2010**, *114*, 10523–10530.
- (77) Tolbert, L. M. Private communication.
- (78) Ando, K.; Hynes, J. T. *J. Mol. Liq.* **1995**, *64*, 25–37.
- (79) Ando, K.; Hynes, J. T. *J. Phys. Chem. B* **1997**, *101*, 10464–78.
- (80) Ando, K.; Hynes, J. T. *Faraday Discuss.* **1995**, *102*, 435–441.
- (81) Ando, K.; Hynes, J. T. *J. Phys. Chem. A* **1999**, *103*, 10398–408.
- (82) Marcus, R. A. *J. Phys. Chem.* **1968**, *72*, 891–899.
- (83) Marcus, R. A. *J. Am. Chem. Soc.* **1969**, *91*, 7224–7225.
- (84) Marcus, R. A. *Faraday Discuss.* **1982**, *74*, 7–15.
- (85) Marcus, R. A.; Sutin, N. *Biochim. Biophys. Acta* **1985**, *811*, 265–322.
- (86) Kuznetsov, A. M.; Ulstrup, J. *Russ. J. Electrochem.* **2004**, *40*, 1010–1018.
- (87) Kornyshev, A. A.; Kuznetsov, A. M.; Spohr, E.; Ulstrup, J. *J. Phys. Chem. B* **2003**, *107*, 3351–3366.
- (88) Hynes, J. T. *Nature* **2007**, *446*, 440–443.
- (89) Ando, K.; Hynes, J. T. *Chem. Phys.* **1999**, *110*, 381–430.
- (90) Kiefer, P. M.; Hynes, J. T. *J. Phys. Chem. A* **2002**, *106*, 1850–1861.
- (91) Kiefer, P. M.; Hynes, J. T. *J. Phys. Chem. A* **2002**, *106*, 1834–1849.
- (92) Kiefer, P. M.; Hynes, J. T. *Solid State Ionics* **2004**, *168*, 219–224.
- (93) Kiefer, P. M.; Hynes, J. T. *J. Phys. Chem. A* **2004**, *108*, 11793–11808.
- (94) Kiefer, P. M.; Hynes, J. T. *J. Phys. Chem. A* **2003**, *107*, 9022–9039.
- (95) Kiefer, P. M.; Hynes, J. T. *Isr. J. Chem.* **2004**, *44*, 171–184.
- (96) Kiefer, P. M.; Hynes, J. T. *J. Phys. Chem. A* **2004**, *108*, 11809–11818.
- (97) Cohen, A. O.; Marcus, R. A. *J. Phys. Chem.* **1968**, *72*, 4249–4256.
- (98) Hammet, L. P. *Trans. Faraday Soc.* **1938**, *34*, 156–165.
- (99) Taft, R. W. *J. Am. Chem. Soc.* **1952**, *74*, 3120–3128.
- (100) Taft, R. W.; Lewis, I. C. *J. Am. Chem. Soc.* **1958**, *80*, 2441.
- (101) Hansch, C.; Leo, A.; Taft, R. W. *Chem. Rev.* **1991**, *91*, 165–195.
- (102) Agmon, N.; Rettig, W.; Groth, C. *J. Am. Chem. Soc.* **2002**, *124*, 1089–1096.
- (103) Westheimer, F. H. *Chem. Rev.* **1961**, *61*, 265–273.
- (104) Bell, R. P. *The Proton in Chemistry*, 2nd ed.; Chapman and Hall: London, 1973.
- (105) Barroso, M.; Arnaut, L. G.; Formosinho, S. J. *J. Photochem. Photobiol. A* **2002**, *154*, 13–21.
- (106) Pines, E. In *Isotope Effects in Chemistry and Biology*; Kohen, A., Limbach, H.-H., Eds.; CRC Taylor & Francis: Boca Raton, FL, 2006; pp 451–464.
- (107) Krishnan, R.; Lee, J.; Robinson, G. W. *J. Phys. Chem. A* **1990**, *94*, 6365–6367.
- (108) *Computer Simulations of Isotope Effects in Enzyme Catalysis*; Warshel, A., Olsson, M. H. M., Eds.; Marcel Dekker: Boca Raton, London, NY, 2006; pp 621–644.